VESPA
Vaso per Esperimenti Su Plasmi ed Altro

Andrea Grossutti, mat. 1237344
Alessandro Lovo, mat. 1236048
Leonardo Zampieri, mat. 1237351

December 17, 2019

1 Aims

Study the *Vespa* experimental apparatus, and in particular:

- Model the vacuum system behavior, finding the characteristic parameters;
- Obtain the current-voltage and the current-temperature characteristics curves of the filament;
- Draw the voltage-current characteristics curves of the gas discharge, enhancing their behavior as varying pressure;
- Find the Paschen curve, both in DC and RF condition;
- Measurement of plasma parameters through a Langmuir probe, both in stationary conditions and via ionic-sonic wave propagation.

2 Vacuum system

The vacuum inside the VESPA vessel (a cylindrical vessel, with a length of $\sim$ 80cm and a radius of $\sim$ 20cm: $V \sim 0.1\text{m}^3$) is obtained and kept thanks to a rotary pump and a turbomolecular pump. The vessel is not perfectly isolated and some small leaks affect the vacuum keeping. To study this phenomena, the vessel has been taken to a low pressure ($\sim 6 \cdot 10^{-5}$mbar) and all the valves around have been closed. Isolating the chamber from the pumping system one can measure (thanks to a ionization pressure gauge) the pressure in the vessel as function of time. Effects as leaks and degasing contribute to an inflow in the chamber $F_0(p)$ that in principle could depend on the pressure. Assuming instead F_0 constant, its value can be estimated through a linear fit on the data: $P = a + b \cdot t$, $F_0 = V \cdot b$.

Considering the reaction time, the slowness of the ionization gauge in stabilizing and the pressure oscillations, the errors are estimated as 5% on the pressure and a 0.5s error on the time.

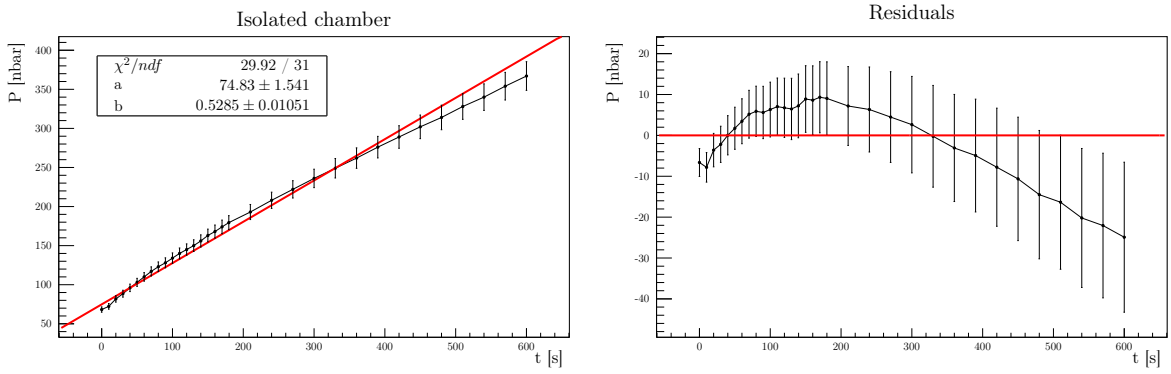

Figure 1: Presure increasing in the chamber

As can be seen from fig 1 there is an evident trend in the residuals, proving that F_0 cannot be assumed constant throughout all the explored range of pressures. A simple way to correct this is to

consider a low pressure regime and a high pressure one: the limit should be put where the trend in the residuals inverts, i.e. around 200nPa.

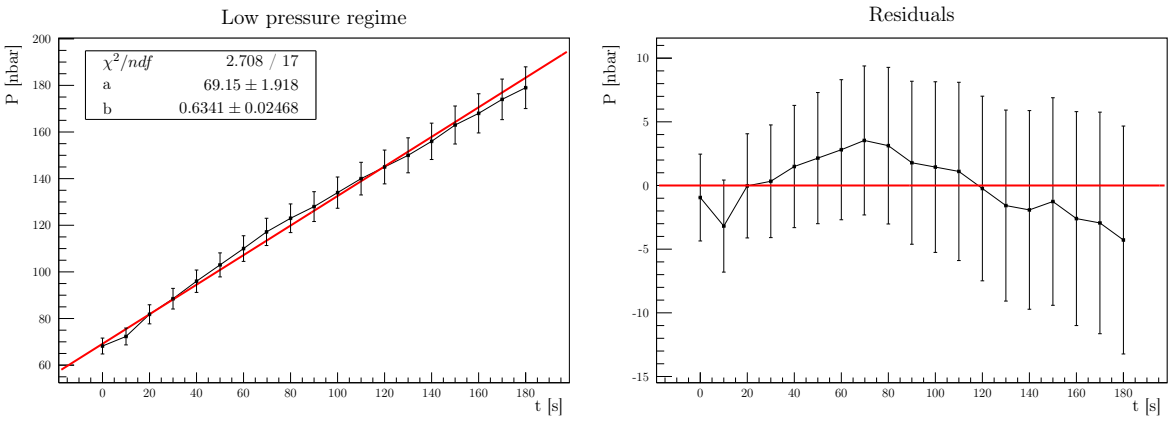

Figure 2: Low pressure regime

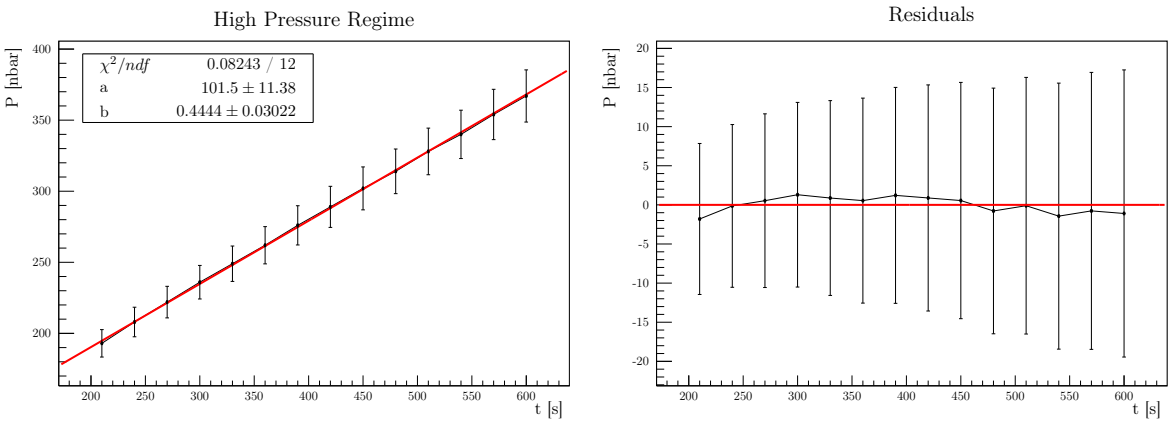

Figure 3: High pressure regime

Splitting the high pressure area and the low pressure area, performing two different fits and assuming a 5% error on the volume, the inflow can be estimated as:

$$F_0^{\text{low}} = (6.4 \pm 0.4) \cdot 10^{-6} \text{Pa}\,\text{m}^3/\text{s}, \quad F_0^{\text{high}} = (4.5 \pm 0.4) \cdot 10^{-6} \text{Pa}\,\text{m}^3/\text{s}$$

Subsequently, the valve has been opened connecting the chamber to the pumping system. An exponential decay of the pressure is expected: $P(t) = (P_i - P_0)\exp\big(-t/\tau\big) + P_0$, where P_i is the starting pressure and P_0 the asymptotic pressure.

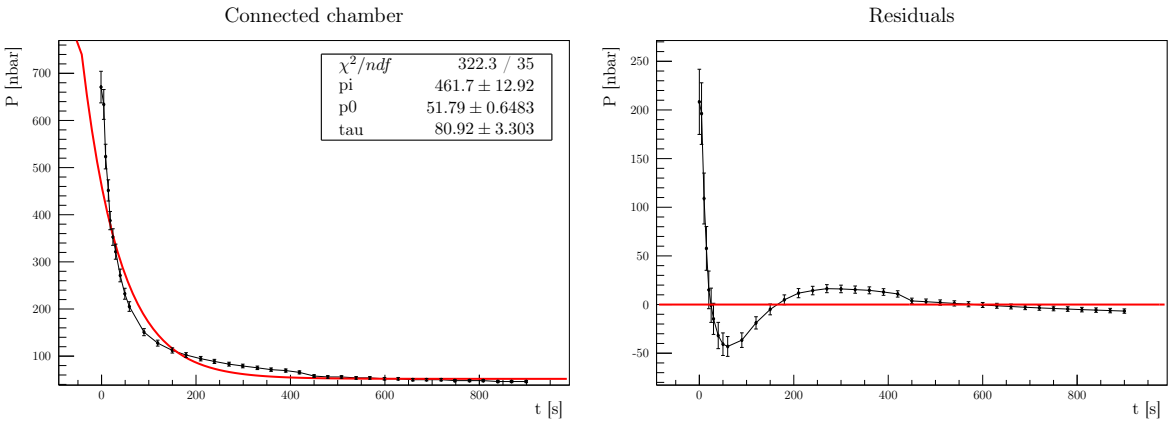

Figure 4: Presure decreasing in the chamber

As can be seen from fig 4, similarly as what seen before, the result are not acceptable and as before two regimes can be distinguished. For coherence the same limit as before has been used.

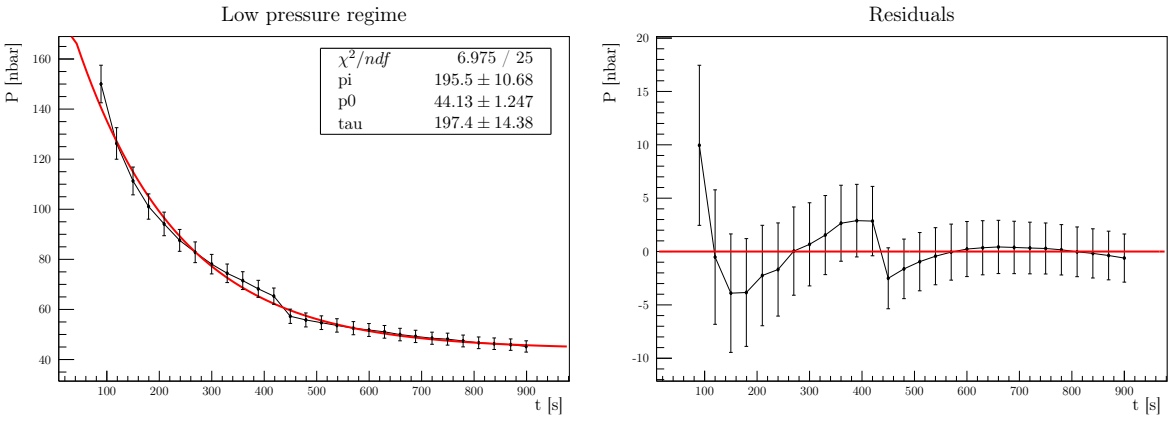

Figure 5: Low pressure regime

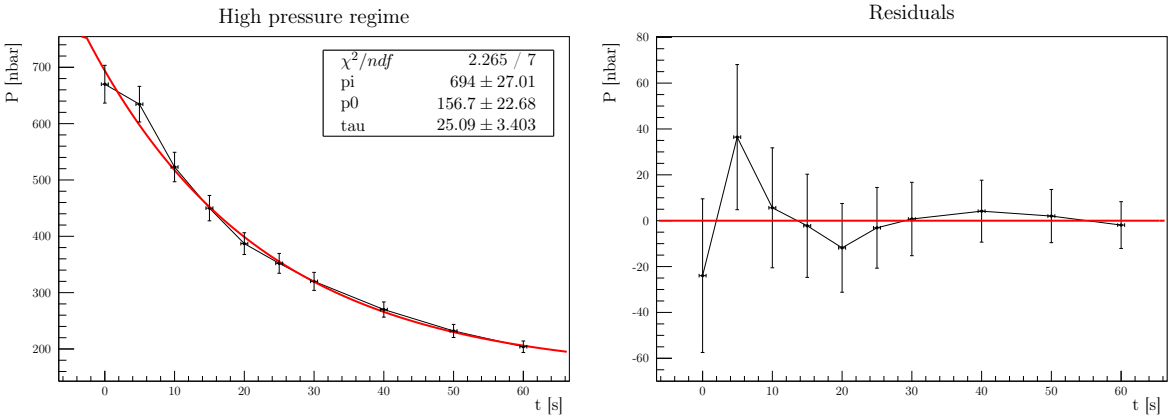

Figure 6: High pressure regime

Performing two different exponential fits there are still trends in the residuals, but now the result is acceptable. From the values of τ and P_0 the effective pumping speed S_e, the inflow F_0 and, given the nominal value of the pumping speed $S = 33$l/s, the conductance of the chamber-pump connection C can be estimated.

regime	$S_e = V/\tau$ [l/s]	$F_0 = P_0 \cdot S_e$ [Pa m^3/s]	$C = 1/(1/S_e - 1/S)$ [l/s]
low pressure	0.51 ± 0.04	$(2.2 \pm 0.2) \cdot 10^{-6}$	0.52 ± 0.05
high pressure	4.0 ± 0.6	$(2 \pm 1) \cdot 10^{-5}$	4.6 ± 0.7

Table 1: Vacuum parameters

In the low pressure regime the two estimates of F_0 are not compatible but still comparable, on the other hand at high pressure the two estimates differ by an order of magnitude. By comparing the nominal value of the pumping speed with S_e one can deduce that most of the pump potential is wasted by a very low conductance connection.

3 Voltage-Current characteristic of the filament

The filament inside the vessel is a tungsten filament with diameter $2r \sim 0.25$mm and length $L \sim 10$cm. Combining Ohm law and emissivity rules, a theoretical characteristic curve can be obtained:

$$V = \frac{A^{10/7} L}{\pi^{13/7} r^{23/7} (2\epsilon\alpha)^{3/7}} \cdot I^{13/7}$$

where ϵ is the effective emissivity, α the StefanBoltzmann constant and A a the resistivity proportional constant, such that the resistivity ρ can be expressed as function of the temperature T as

$$\rho(T) = AT^{6/5}$$

Pumping the vessel to a low pressure (~ 2), the voltage-current characteristic curve of the filament has been measured, producing the following data:

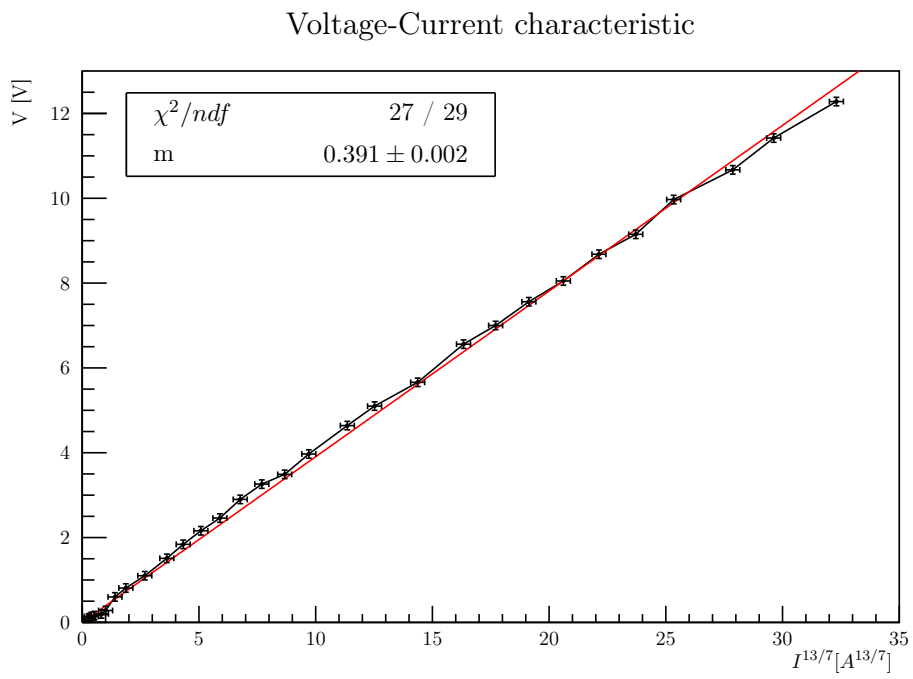

Figure 7: Voltage-Current characteristic for a filament; errors has been chosen as $0.3A^{13/7}$ and $0.1V$, due to the low sensibility of the measure system.

Fitting the data with a $V \propto I^{13/7}$, the following parameters are found:

$$V = mI^{13/7} \tag{1}$$

$$m = (0.391 \pm 0.002)\mathrm{V} \cdot \mathrm{A}^{-13/7} \tag{2}$$

which lead to a value of

$$\epsilon \sim 0.2$$

The χ^2 confirm the meaningfulness of the fit; moreover, the effective emissivity have a value similar to the typical ones.

Finally, the estimated filament temperature as a function of the driven current can be found:

$$T = \underbrace{\frac{A^{5/14}}{\pi^{5/7} r^{15/14} (2\epsilon\alpha)^{5/14}}}_{k} \cdot I^{5/7} \qquad \text{with } k \sim 811\text{K} \cdot \text{A}^{-5/7}$$

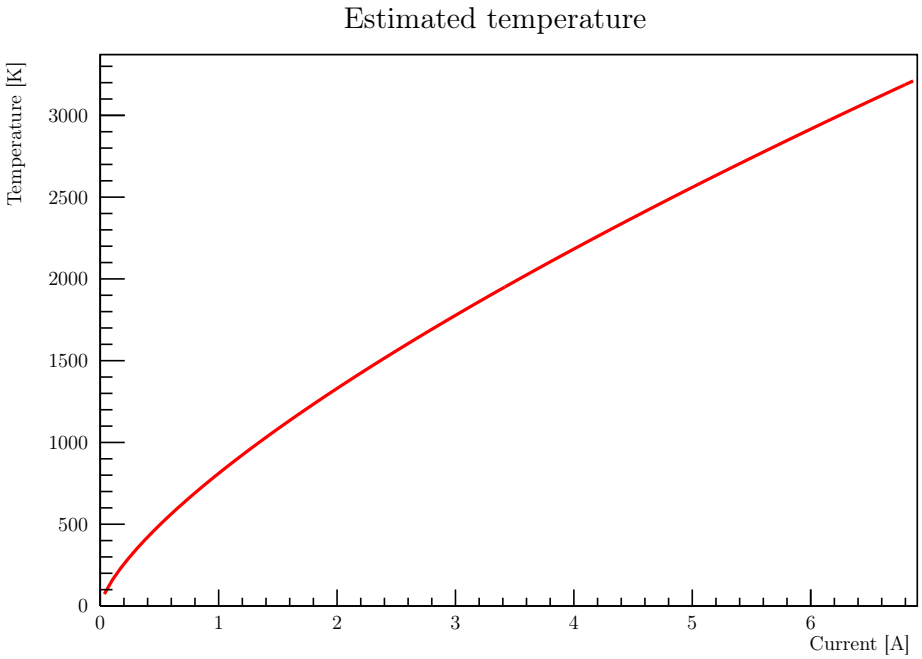

Figure 8: Projection of the filament temperature as function of the current

4 DC analysis of the plasma

4.1 Voltage-current characteristics of the discharge

By polarizing the filament with respect to the grid (grounded) a discharge in the plasma can be achieved. By measuring the polarization voltage on the power supply (0.1 V error) and the plasma current via the voltage fall on a resistor $R_{shunt} = (1 \pm 0.03)\Omega$, the discharge V-I curve can be studied. In particular the breakdown voltage is clearly visible.

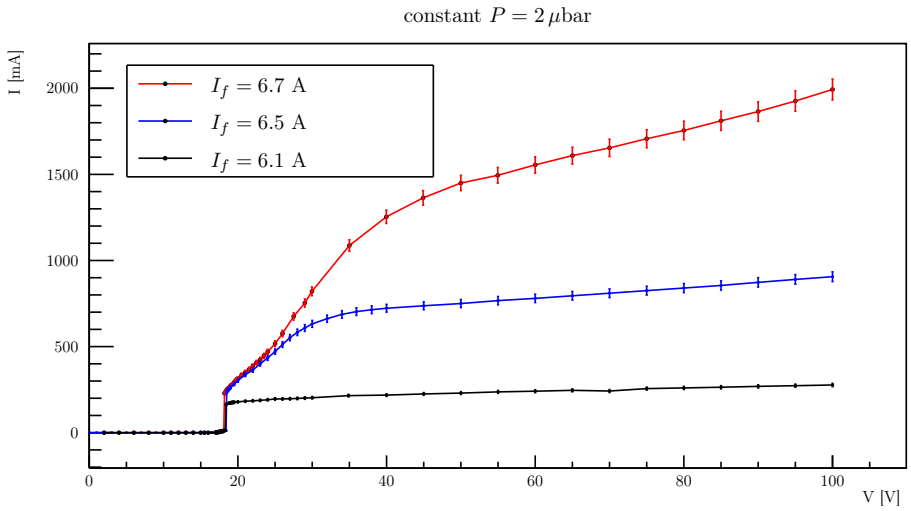

Figure 9: V-I characteristics of the discharge at constant pressure P, varying the filament current I_f

As can be seen from fig 9 changing I_f doesn't change the breakdown voltage, but changes the the characteristics of the plasma once it is ignited. This effect is due to the thermoionic emission of the filament and is explained by Richardson law:

$$I = \Sigma A T^2 \exp\left(-\frac{e\Phi}{k_B T}\right)$$

where $A = 7 \cdot 10^5 \mathrm{A/m^2K^2}$, $\Phi = 4.55\mathrm{V}$ and Σ is the surface of the filament

compute Σ

By using the previous found relation between the temperature and the filament current $T = k \cdot I_f^{5/7}$ the expected plasma current can be computed.

Ma In Richardson non c'e' nessuna dipendenza dalla tensione di polarizzazione... inoltre in che regime di plasma siamo? Bagliore o arco?

By studying instead the V-I characteristics varying the Argon pressure one obtains the results in fig 10, where it is visible the influence of the pressure on the breakdown voltage, effect that can be better understood building the experimental Paschen curve.

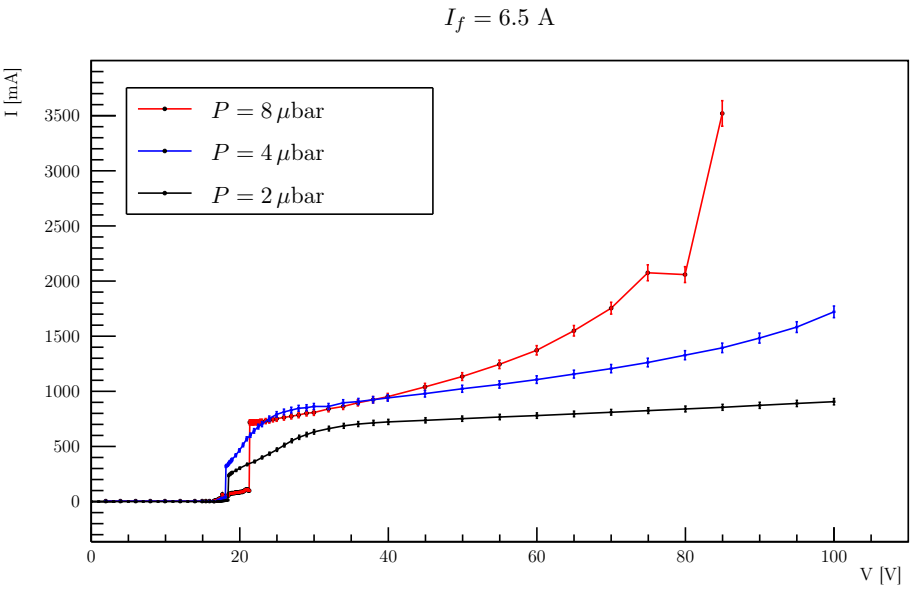

Figure 10: V-I characteristics of the discharge at constant filament current I_f, varying the pressure P

4.2 Paschen curve in DC condition

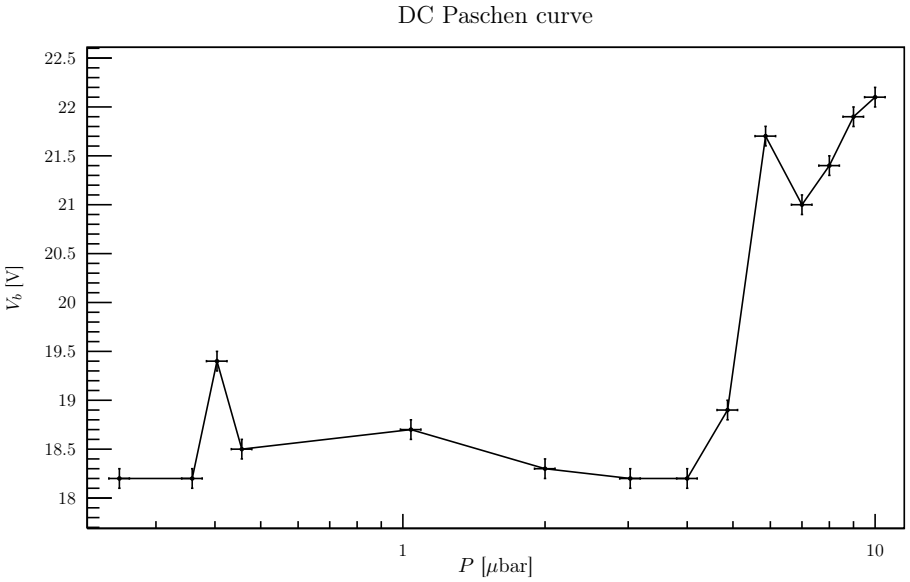

Figure 11: Experimental Paschen curve: breakdown voltage vs P

As can be seen from fig 11 the curve is quite noisy so a fit with the theoretical formula of the Paschen curve would fail. On the other hand the Paschen's minimum is clear to be between 3 and 4 µbar.

5 Paschen curve in radiofrequency condition

Inside VESPA a magnetic antenna is provided, which allow to induce a plasma through radiofrequency waves that, coupling with gas electrons, excite them and generate the discharge.

The antenna is powered through a RF generator and a RLC circuit; firstly, the response of the circuit is studied. Keeping fixed the generator power and varying the frequency, through an oscilloscope the peak-to-peak amplitude of the wave downstream the circuit is measured. The result is a typical resonance courve (fig. 12).

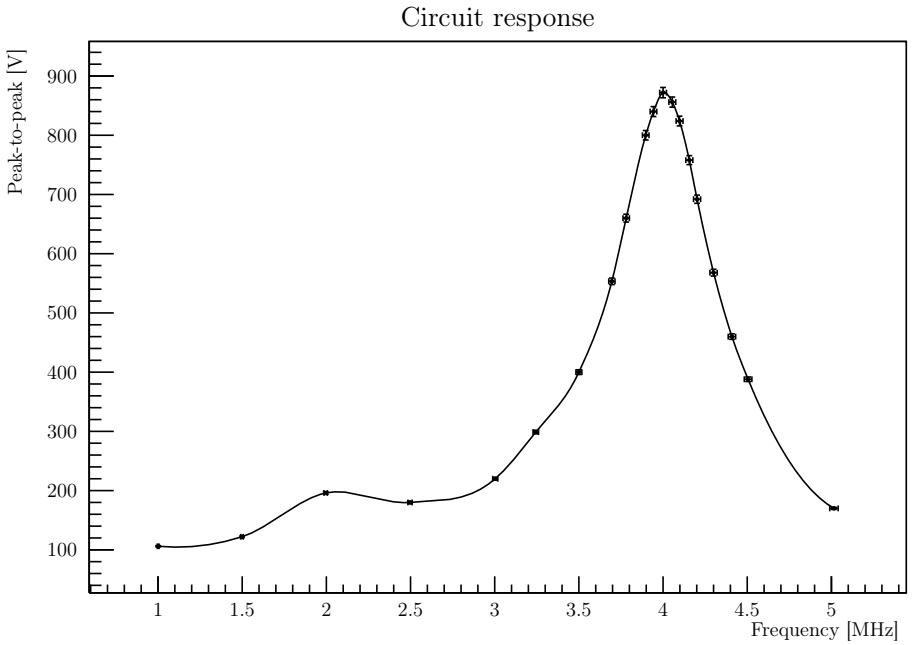

Figure 12: Peak-to-peak amplitude downstream the circuit, varying the wave frequency. From the oscillation in the measurements and the instrumentation sensibility, the errors has been estimated at 5‰ in the frequencies and 1% in voltages.

From the fig. 12 the maximum can be detected: it is around 4MHz. Therefore the operation area is identified in the range 3–4MHz, when the amplitude is high and increasing with the frequency.

Varying the pressure in the vessel, the breakdown voltage trend can be studied. For each pressure, the frequency has been increased until the discharge took place (it's a clearly visible phenomena, so the discrimination has been done visually), and the peak-to-peak voltage in the breakdown point has been measured. The result is the Paschen curve in fig. 13.

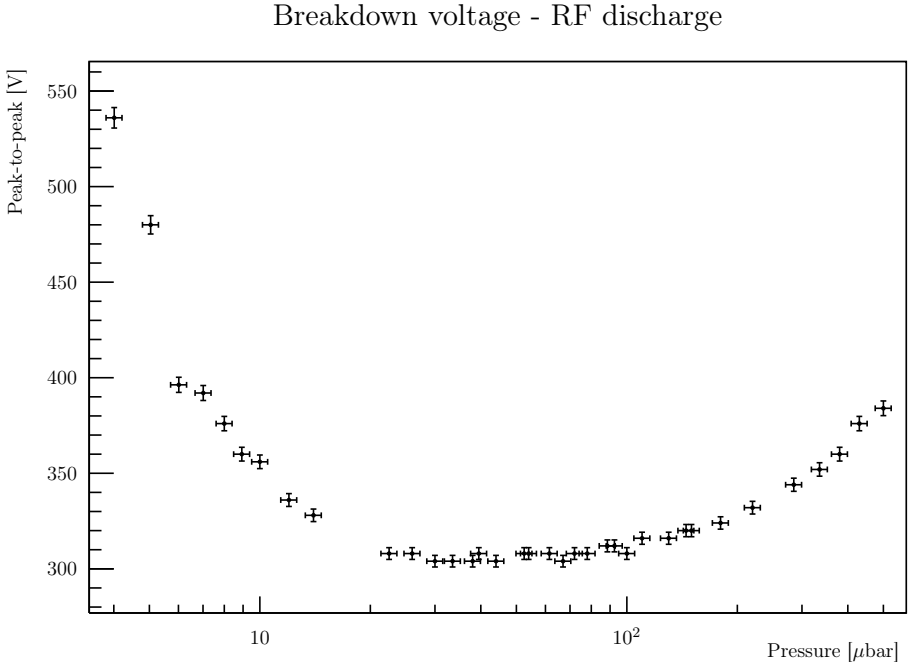

Figure 13: Radiofrequency Paschen curve. From the oscillation in the measurements and the instrumentation sensibility, the errors has been estimated at 5% in the pressures and 1% in voltages.

As can be seen from the plot, the minimum of the Paschen curve in radiofrequency condition is very large: the optimal area can be identified in the range:

$$3\text{–}7 \cdot 10^{-5}\text{bar}$$